A Systematic Way of Approximating Gain Recovery Dynamics in SOAs

Malin Premaratne, *Senior Member, IEEE,* , Govind P. Agrawal, *Fellow, IEEE, Fellow, OSA* and Dragan Nesic, *Fellow, IEEE*

***Abstract*— Short picosecond pulse propagation in semiconductor optical amplifiers (SOAs) has been widely studied for applications in optical signal processing and optical communications areas. Even though it is possible to fully numerically integrate differential equations describing the dynamics of SOAs, such implementations may not provide adequate insight into the device operation. We propose a systematic way to construct analytical solutions for the gain recovery dynamics of SOAs with excellent agreement with numerically integrated results. Our approach is a formalization of an heuristic technique used by researchers in the past for constructing an approximate analytical solution of carrier dynamics in a two level system by first treating stimulated emission process as instantaneous. Just after the stimulated emission-induced carrier depletion, it is assumed in this approach that carriers will replenish themselves to the initial steady-state population through carrier injection, with a carrier-recovery lifetime. The main contribution of this work is to put this heuristic approach into a firm theoretical base so that approximate analytical solutions for carrier recovery dynamics for different variants of SOA models can be systematically constructed. We derive analytical solutions for modal signal gain and pulse energy gain at an arbitrary point of the SOA waveguide. Surpassing previous work in this area, we also show that it is possible to construct analytical solutions to described gain recovery dynamics when waveguide attenuation is not negligible.**

***Index Terms*— Semiconductor Optical Amplifiers, Gain Recovery Dynamics, Approximate Analytical Solution.**

I. Introduction

SEMICONDUCTOR optical amplifiers (SOAs) are increasingly used in optical signal processing applications in all-optical integrated circuitry [1], [2]. The effectiveness of SOAs in all-optical integrated circuitry results from their high-gain coefficient and low saturation power [3], [4]. In addition, SOAs are widely used for constructing functional devices such as nonlinear loop mirrors [5], [6], clock-recovery circuits [7], [8], pulse-delay discriminators [9]–[11] and logic operations [12], [13]. Device engineering and performance optimization requires a good quantitative understanding of active SOAs used in above functional blocks. Also, most of the engineering optimization methods require the ability to repeatedly estimate the operation of a devices when small parametric changes are made in functional blocks. All this reasoning justifies having simple but quantitatively accurate models for SOAs with the ability to capture significant spatial and temporal features.

Pulse amplification in two-level media have been studied extensively in the past [14], [15]. Frantz and Nodvik [16] have pioneered the description of pulse amplification based on the the energy of the pulse and extraction efficiency in two level systems. They used rate equations to calculate the amplifier gain using the input pulse energy (i.e. without taking the specific details about the pulse shape). Their technique relies on the assumption that the stimulated-emission-induced carrier depletion due to a short pulse (i.e a pulse whose full width at half maximum (FWHM) is much smaller than carrier lifetime) can be considered instantaneous. Just after the stimulated emission induced carrier depletion, carriers will replenish themselves to the initial steady-state population through carrier injection, with a rate equal to the carrier-recovery lifetime. Siegman [17] showed how these results can be re-casted using amplified pulse energies (i.e. output pulse energies) and derived a transcendental equation describing the input, output pulse energies and the energy supplied to the two-level medium. Premaratne *et al.* [10] demonstrated how to extend the Frantz-Nodvik [16] technique to describe counter-propagating short pulse trains in SOAs. Their simulations showed that spatial carrier distribution profile can also be described accurately during pulse pulse transient period and beyond. The impact on amplified spontaneous emission (ASE) noise on gain recovery dynamics in SOA within the Frantz-Nodvik [16] framework was carried out for polarization-insensitive and polarization-sensitive SOAs in [11] and [18], respectively.

In this paper, we propose a systematic way to conduct a Frantz-Nodvik type analysis [16] for gain recovery dynamics in SOAs using multiple-scales techniques [19], [20]. The main contribution of this work is to put heuristic arguments onto a firm theoretical base so that approximate analytical solutions for carrier recovery dynamics for different variants of SOA models can be systematically constructed. Surpassing previous work in this area, we also show that it is possible to construct analytical solutions to describe gain recovery dynamics when waveguide attenuation is not negligible. In Section II, we derive the integro-differential equation governing gain recovery dynamics of a SOA when a short optical pulse interacts with the gain medium. In Section III, we derive an approximate analytical solution for gain recovery dynamics of an SOA when

Manuscript received June 15, 2007; accepted October 15, 2007.

M. Premaratne is with the Advanced Computing and Simulation Laboratory (AXL), Department of Electrical and Computer Systems Engineering, Monash University, Clayton, Victoria 3800, Australia. email: malin@eng.monash.edu.au. He is currently visiting The Institute of Optics, University of Rochester, New York.

G. P. Agrawal is with The Institute of Optics, University of Rochester, Wilmot 206, Rochester, New York 14627-0186 USA. email: gpa@optics.rochester.edu

D.Nesic is with the Department of Electrical and Electronic Engineering, The University of Melbourne, Parkville, 3052, Victoria, Australia. email:d.nesic@unimelb.edu.au

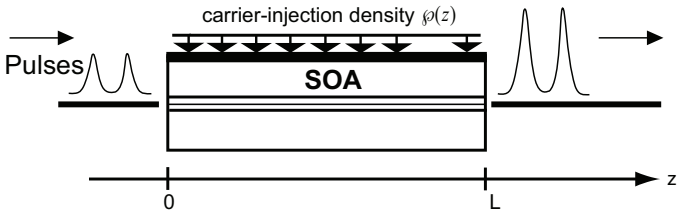

Fig. 1. Schematic diagram of the SOA and the coordinate system used in the analysis.

waveguide loss is negligible. This work is then extended to lossy waveguides in Section IV. Comparing results generated using detailed numerical integration, a detailed analysis of the validity of the proposed method in carried out in Section V. We conclude this paper in Section VI.

II. Integro-Differential Equation Governing the Gain Recovery Dynamics of a SOA

In this section we show that gain recovery dynamics of an SOA can be described completely using a single integro-differential equation. In this derivation, we do not discard the waveguide attenuation but limit our analysis to pulses with FWHM in the picosecond range. A main implication of this assumption is that we do not need to take into account carrier heating and intra-band relaxation processes in our analysis, considerably simplifying algebraic structure of the final solution.

Fig. 1 shows a schematic diagram of the optical semiconductor amplifier (SOA) studied in this paper. We use a coordinate axis z along the SOA propagation axis with its origin at the left facet. We assume that the length of SOA is given by L and the carrier are injected to SOA medium with the carrier injection-density $\wp(z)$. Optical pulses enter the SOA from its left facet and leave SOA from its right facet. We do not consider any back propagating waves along the SOA either due to partial reflections or amplified spontaneous emission events. Even though relaxing them limit the accuracy of the proposed analysis, decades of research work in SOAs have shown that in many instances, such assumptions only introduce second order effects to the analysis presented here [11], [18]. Therefore, without loss of generality, we limit our analysis to the above constrained system for clarity and algebraic simplicity.

Suppose $I_{T_w}(t)$ is the intensity profile of an optical pulse with arbitrary shape but with a FWHM of T_w and energy, E_g. The latter assumption implies

$$E_g = A \int_{-\infty}^{+\infty} I_{T_w}(t) dt \tag{1}$$

where A is the mode area of the SOA active region. Due to the short pulse assumption, the carrier lifetime, τ_e, of the semiconductor medium is much greater than the FWHM of the optical pulse (i.e. $\tau_e \gg T_w$). The dynamic response of the SOA is given by [3]:

$$\frac{\partial}{\partial z} I(z,t) + \frac{1}{v_g} \frac{\partial}{\partial t} I(z,t) = g(z,t) I(z,t) - \alpha I(z,t) \tag{2}$$

$$\frac{\partial}{\partial t} N(z,t) = \wp(z) - \frac{N(z,t)}{\tau_e} - g(z,t) \frac{\lambda I(z,t)}{hc} \tag{3}$$

where t is time, z is distance along the SOA measured from the left facet, $I(z,t)$ is the intensity of the optical signal along the SOA, $N(z,t)$ is the carrier density along the SOA, α is the loss coefficient, Γ is the mode confinement factor, a is the differential gain coefficient, $g(z,t) = \Gamma a \left(N(z,t) - N_0\right)$, $\wp(z)$ is the current injection density along the SOA, λ is the mean operating wavelength, c is the speed of light in vacuum and h is the Plank's constant. To make subsequent analysis easier, we make the coordinate transformations $\xi = z$ and $\tau = t - z/v_g$ so that we are in a reference plane that moves with the forward propagating pulse, giving following coordinate transformed equations

$$\frac{\partial}{\partial \xi} I(\xi,\tau) = g(\xi,\tau) I(\xi,\tau) - \alpha I(\xi,\tau) \tag{4}$$

$$\frac{\partial}{\partial \tau} N(\xi,\tau) = \wp(\xi) - \frac{N(\xi,\tau)}{\tau_e} - g(\xi,\tau) \frac{\lambda I(\xi,\tau)}{hc} \tag{5}$$

Solving (4) as an initial value problem results in

$$I(\xi,\tau) = I_{T_w}(\tau) \exp\left(\int_0^{\xi} \left(g(\xi,\tau) - \alpha\right) \, d\xi \right) \tag{6}$$

It is very clear from the structure of (6) that subsequent calculations can be simplified by introducing a new variable $h(\xi,\tau)$ with the following definition

$$h(\xi,\tau_n) = \int_0^{\xi} g(\xi,\tau) \, d\xi \tag{7}$$

where ξ is going to be in the interval $[0, L]$, L is the SOA length and normalized time, τ_n is defined using the SOA cavity transit time, $t_{cav} = L/v_g$ as $\tau_n = \tau / t_{cav}$. Substitution of (7) to (5) gives us a single integro-differential equation describing the gain recovery dynamics of a SOA

$$\begin{aligned} \frac{\partial}{\partial \tau_n} h(\xi,\tau_n) &= \epsilon \left(h_{\wp} - h(\xi,\tau_n)\right) \\ &\quad -\beta(\tau_n) \left(\exp\left(h(\xi,\tau_n) - \alpha\xi\right) - 1\right) \\ &\quad -\beta(\tau_n) \left(\alpha \int_0^{\xi} \exp\left(h(\xi,\tau_n) - \alpha\xi\right) \, d\xi \right) \end{aligned} \tag{8}$$

where $\epsilon = t_{cav}/\tau_e$, $\beta(\tau_n) = \Gamma a \lambda I_{Tw}(t_{cav}\tau_n) t_{cav}/hc$ and

$$h_{\wp}(\xi) = \int_0^{\xi} \left(\tau_e \Gamma a \wp(\xi) - \Gamma a N_0\right) \, d\xi \tag{9}$$

This equation can be numerically integrated very accurately using well known integro-differential equation techniques [21]. However, such numerical analysis does not provide adequate insight into device operation because essential dynamical features and parameters are not readily observable. Even though it is not possible to analytically solve (8), we seek an approximate solution capturing the essential variables governing the dynamics of this gain recovery equation.

III. Analytical Approximation of Gain Recovery Dynamics When Waveguide Loss is Negligible

When loss is negligible compared with gain, we can substitute $\alpha = 0$ to (8), leading to the following partial differential equation

$$\frac{\partial}{\partial \tau_n} h(\xi, \tau_n) = \epsilon \left(h_{\wp} - h(\xi, \tau_n)\right) - \beta(\tau_n) \left(\exp\left(h(\xi, \tau_n)\right) - 1\right) \quad (10)$$

Even though it is not possible to analytically solve this equation, we could seek a solution in using multiple-scales analysis technique. The main impetus for such an approach stems from our observation that stimulated emission and carrier recovery has two distinct time scales; fast stimulated transitions associated with the pulse original time $\mathcal{T} = \tau_n$ and slow, carrier recovery time scale associated with slow-time $\mathcal{U} = \epsilon \tau_n$. The underlying idea in the method of multiple scales is to formulate the original problem in terms of these two time-scales from the outset and then to treat the original functional variable as a function of two variables. Even though $\mathcal{T}$ and $\mathcal{U}$ are interdependent, we treat them as separate, independent variables and seek an asymptotic solution in the two dimensional space of $(\mathcal{T}, \mathcal{U})$. Thus, the obtained solution is more general than the solution of the original problem but contains the original solution as a special case. This aspect can be understood by noting that because such an asymptotic solution is valid in the two dimensional region, it will also be valid in any and every path in this region of the $(\mathcal{T}, \mathcal{U})$ space.

Within the multiple-scale description we assume that

$$h\left(\xi, \tau_n\right) \equiv h\left(\xi, \mathcal{T}, \mathcal{U}, \epsilon\right) \quad (11)$$

and express the partial differential operator of τ_n using $(\mathcal{T}, \mathcal{U})$ variables

$$\frac{\partial}{\partial \tau_n} = \frac{\partial}{\partial \mathcal{T}} + \epsilon \frac{\partial}{\partial \mathcal{U}} \quad (12)$$

Substitution of this new partial differential operator to (10) including the new functional definition (11) leads to

$$\frac{\partial}{\partial \mathcal{T}} h\left(\xi, \mathcal{T}, \mathcal{U}, \epsilon\right) + \epsilon \frac{\partial}{\partial \mathcal{U}} h\left(\xi, \mathcal{T}, \mathcal{U}, \epsilon\right) = \epsilon \left(h_{\wp} - h\left(\xi, \mathcal{T}, \mathcal{U}, \epsilon\right)\right) - \beta(\tau_n) \left(\exp\left(h\left(\xi, \mathcal{T}, \mathcal{U}, \epsilon\right)\right) - 1\right) \quad (13)$$

Assuming that ϵ is a small parameter (i.e. $|\epsilon| \ll 1$), we seek an asymptotic solution for the above partial differential equation as a power series expansion of the parameter ϵ

$$h\left(\xi, \mathcal{T}, \mathcal{U}, \epsilon\right) = \sum_{n=0}^{\infty} h_n\left(\xi, \mathcal{T}, \mathcal{U}\right) \epsilon^n \quad (14)$$

Substitution of (14) to (13) and noting that

$$\exp\left(h\left(\xi, \mathcal{T}, \mathcal{U}, \epsilon\right)\right) \approx \exp\left(h_0\left(\xi, \mathcal{T}, \mathcal{U}\right)\right) \left(1 + \epsilon h_1\left(\xi, \mathcal{T}, \mathcal{U}\right) + \cdots\right) \quad (15)$$

we get a partial differential equation as a power series expansion of the small variable ϵ. Because this power series expansion needs to be identically equal to zero, coefficients of each higher order term $\epsilon^n : n = 0, 1, 2, \cdots$ must be equal to zero. Equating the lowest term (i.e. ϵ^0) to zero results in

$$\frac{\partial}{\partial \mathcal{T}} h_0\left(\xi, \mathcal{T}, \mathcal{U}\right) = -\beta(\mathcal{T}) \left(\exp\left(h_0\left(\xi, \mathcal{T}, \mathcal{U}\right)\right) - 1\right) \quad (16)$$

and equating the first order term (i.e. ϵ^1) results in

$$\frac{\partial}{\partial \mathcal{T}} h_0\left(\xi, \mathcal{T}, \mathcal{U}\right) + \frac{\partial}{\partial \mathcal{U}} h_1\left(\xi, \mathcal{T}, \mathcal{U}\right) = \left(h_{\wp} - h_0\left(\xi, \mathcal{T}, \mathcal{U}\right)\right) - \beta(\mathcal{T}) \exp\left(h_0\left(\xi, \mathcal{T}, \mathcal{U}\right)\right) h_1\left(\xi, \mathcal{T}, \mathcal{U}\right) \quad (17)$$

We seek a solution for $h_0\left(\xi, \mathcal{T}, \mathcal{U}\right)$ in 2-space $(\mathcal{T}, \mathcal{U})$ by seeking a solution that satisfy (16) and (17), simultaneously.

It is interesting to note that by adding correction terms of higher orders in ϵ, we could successively improve the accuracy of the approximation. However, due to the algebraic complexity of the resulting terms, a simpler intuitive solution amenable to clear insightful physical interpretation may not be possible. Estimating non-strict upper bounds of (14), we could show that it is possible to achieve arbitrary closeness of solution between the approximation and exact result. However, such rigorous proof is beyond the scope of this paper and will be published elsewhere. Instead, we resort to numerical simulations to show the matching of results within parameter ranges applicable to typical commercially available SOAs.

A. Initial Conditions

We assume that the initial conditions for $h\left(\xi, \mathcal{T}, \mathcal{U}, \epsilon\right)$ is independent of the small-parameter ϵ. This is a reasonable assumption because carrier recovery rate is not going to affect the initial state of the SOA. Let, $h_I(\xi)$ be the initial profile of $h\left(\xi, \mathcal{T}, \mathcal{U}, \epsilon\right)$, enabling us to define the initial conditions of each polynomial coefficient of ϵ

$$h_n\left(\xi, 0, 0\right) = \begin{cases} h_I(\xi) & \text{if} \quad n = 0 \\ 0 & \text{otherwise} \end{cases} \quad (18)$$

B. Analytical Solution of the Equation (16)

Differential equation (16) can be solved by multiplying (16) by the integrating factor $\exp\left(-h_0\left(\xi, \mathcal{T}, \mathcal{U}\right)\right)$ to transform (16) to following form

$$\frac{\partial}{\partial \mathcal{T}} \exp\left(-h_0\left(\xi, \mathcal{T}, \mathcal{U}\right)\right) = \beta(\mathcal{T}) \left(1 - \exp\left(-h_0\left(\xi, \mathcal{T}, \mathcal{U}\right)\right)\right) \quad (19)$$

This equation can be integrated to get

$$h_0\left(\xi, \mathcal{T}, \mathcal{U}\right) = -\ln\left(1 - \left(1 - \exp\left(-h_0\left(\xi, 0, \mathcal{U}\right)\right)\right) \frac{\varphi(\mathcal{U})}{E_\beta(\mathcal{T})}\right) \quad (20)$$

where $\varphi(\mathcal{U})$ is an arbitrary function depending on the slow-time scale, $\mathcal{U}$ and $E_\beta(\mathcal{T})$ is a variable in which the logarithm of it is proportional to the energy of the pulse seen by the gain medium up to the time $\mathcal{T}$

$$E_\beta(\mathcal{T}) = \exp\left(\int_0^{\mathcal{T}} \beta(\mathcal{T})\, d\mathcal{T}\right) \quad (21)$$

C. Analytical Solution of the Equation (17)

If the SOA gain is monitored long time after an optical pulse has left the amplifying medium, there cannot be any dependency of the gain overall gain on small-parameter ϵ. This condition leads to the result that $h_n(\xi,\infty,\infty)=0$ for $n=1,2,\cdots$. Therefore, using (18), it is possible to show by substitution that the following expression is a general solution of (17)

$$\begin{aligned} h_0(\xi,\mathcal{T},\mathcal{U}) = & \\ & h_0(\xi,\mathcal{T},0)\exp(-\mathcal{U}) \\ & +h_\wp(\xi)(1-\exp(-\mathcal{U}))+\vartheta(\mathcal{T})\exp(-\mathcal{U}) \end{aligned} \quad (22)$$

where $\vartheta(\mathcal{T})$ is an arbitrary function depending on the fast-time scale, $\mathcal{T}$. However, (22) must satisfy (16). Enforcing of this constraint enable us to obtain a specific functional form for $\vartheta(\mathcal{T})$ as demonstrated in the next subsection.

D. Modal Signal Gain of SOA

The expressions (20) and (22) for $h_0(\xi,\mathcal{T},\mathcal{U})$ need to be identically equal to each other in the $(\mathcal{T},\mathcal{U})$ space. Considering this, we match the results at initial points in the 2-space. This could be most conveniently done by calculating $\exp(h_0(\xi,0,0))$ for (20)

$$\exp(h_0(\xi,0,0)) = \frac{1}{1-(1-\exp(-h_I(\xi))\varphi(0))} \quad (23)$$

and (22)

$$\exp(h_0(\xi,0,0)) = \exp(h_I(\xi))\exp(\vartheta(0)) \quad (24)$$

Equations (23) and (24) match if

$$\varphi(0)=1 \text{ and } \vartheta(0)=0 \quad (25)$$

However, from (22) we can write

$$\begin{aligned} \exp(h_0(\xi,\mathcal{T},\mathcal{U})) &= \exp(h_0(\xi,\mathcal{T},0)\exp(-\mathcal{U})) \\ &\quad \times\exp(h_\wp(\xi)(1-\exp(-\mathcal{U}))) \\ &\quad \times\exp(\vartheta(\mathcal{T})\exp(-\mathcal{U})) \end{aligned} \quad (26)$$

and use (25) to obtain following expression for $h_0(\xi,\mathcal{T},0)$ from (20)

$$h_0(\xi,\mathcal{T},0) = -\ln\left(1-\frac{(1-\exp(-h_I(\xi)))}{E_\beta(\mathcal{T})}\right) \quad (27)$$

substitution of this to (26) gives us the following expression for modal gain along the SOA with both spatial and temporal variables

$$\begin{aligned} \exp(h_0(\xi,\mathcal{T},\mathcal{U})) &= \exp(h_\wp(\xi)) \\ &\times\left(\frac{\exp(\vartheta(\mathcal{T})-h_\wp(\xi))}{1-(1-\exp(-h_I(\xi)))/E_\beta(\mathcal{T})}\right)^{\exp(-\mathcal{U})} \end{aligned} \quad (28)$$

However, to fully characterize the gain evolution from (28), we need to find the functional form of $\vartheta(\mathcal{T})$ with respect the fast time scale, $\mathcal{T}$. As described before, the underlying idea in the method of multiple scales is to formulate the original problem in terms of two-space, $(\mathcal{T},\mathcal{U})$ from the outset and make the resulting asymptotic solution is valid in a two dimensional region, enclosing the original domain. Because of the constraints set in solving the problem in this enclosing region in the two-space $(\mathcal{T},\mathcal{U})$, it will also be valid in any and every path in this region of the $(\mathcal{T},\mathcal{U})$ space. Therefore, to calculate the specific functional form of $\vartheta(\mathcal{T})$, we seek a path in two-space where $\mathcal{U}$ is identically zero. In such a path, we can evaluate the partial derivative of (28) to get

$$\begin{aligned} \frac{\partial}{\partial\mathcal{T}}h_0(\xi,\mathcal{T},\mathcal{U})\Big|_{\mathcal{U}=0} &= \frac{d}{d\mathcal{T}}\vartheta(\mathcal{T}) \\ &\quad -\beta(\mathcal{T})\frac{(1-\exp(-h_I(\xi)))/E_\beta(\mathcal{T})}{1-(1-\exp(-h_I(\xi)))/E_\beta(\mathcal{T})} \end{aligned} \quad (29)$$

Substituting (29) and (28) to (16), we can derive the following differential equation for the unknown variable $\vartheta(\mathcal{T})$

$$\frac{d}{d\mathcal{T}}\vartheta(\mathcal{T}) = \beta(\mathcal{T})\frac{(1-\exp(\vartheta(\mathcal{T})))}{1-(1-\exp(-h_I(\xi)))/E_\beta(\mathcal{T})} \quad (30)$$

Multiplying (30) by $\exp(-\vartheta(\mathcal{T}))$ and noting that

$$\begin{aligned} &\frac{\beta(\mathcal{T})E_\beta(\mathcal{T})}{E_\beta(\mathcal{T})-(1-\exp(-h_I(\xi)))} \\ &\qquad \equiv \frac{d}{d\mathcal{T}}\ln(E_\beta(\mathcal{T})-(1-\exp(-h_I(\xi)))) \end{aligned} \quad (31)$$

we can get the following general solution for (30)

$$\exp(-\vartheta(\mathcal{T})) = 1-C\times(E_\beta(\mathcal{T})-(1-\exp(h_I(\xi)))) \quad (32)$$

where C is a constant that need to be determined using the initial condition (25) of $\vartheta(0)$. Substitution of $\mathcal{T}=0$ to results in $C=0$ and hence the fast-time $\mathcal{T}$ dependency of $\vartheta(\mathcal{T})$ becomes

$$\vartheta(\mathcal{T}) = 0 \quad (33)$$

leading to following expression for the modal signal gain at time $(\mathcal{T},\mathcal{U})$ and at distance ξ

$$\begin{aligned} \exp(h_0(\xi,\mathcal{T},\mathcal{U})) &= \exp(h_\wp(\xi)(1-\exp(-\mathcal{U}))) \\ &\quad \times(1-(1-\exp(-h_I(\xi)))/E_\beta(\mathcal{T}))^{-\exp(-\mathcal{U})} \end{aligned} \quad (34)$$

In the next subsection, we use this expression to calculate the energy gain seen by the pulse as it propagates through the amplifier.

E. Energy Gain of SOA

One significant result of the analysis so far is that the signal-gain evolution is not directly related to the pulse shape but to the energy, $E_P(\mathcal{T})$, which it presents to the gain medium up to time $\mathcal{T}$

$$E_P(\mathcal{T}) = \frac{hcA}{\Gamma a\lambda}\ln(E_\beta(\mathcal{T})) \quad (35)$$

As clearly seen in the signal gain evolution expression (34), the quantity $E_\beta(\mathcal{T})$ drives the signal gain evolution of the SOA. It is useful to have an alternative expression for (35) based on the initial conditions of the material media and pulse (i.e. $h_I(\xi)$ and $\beta(\mathcal{T})$). Siegman [17] was the first person to calculate such expression for the energy for the limiting case $\mathcal{T}\to\infty$. We generalize his results in this section by using a new strategy to calculate $E_P(\mathcal{T})$ for arbitrary time value $\mathcal{T}$. Our approach relies on the self-consistent argument that overall gain of an SOA should be invariant if we introduce a fictitious internal boundary at an arbitrary point in the SOA medium.

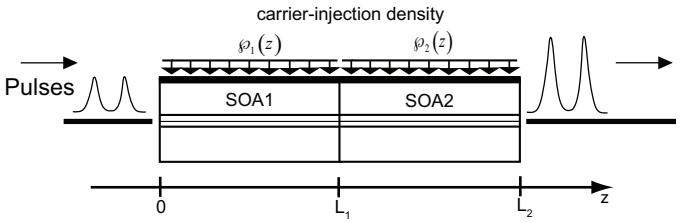

Fig. 2. Introduction of a fictitious boundary at $\xi = L_1$ to view a SOA as a gain-block made-up of two cascaded gain blocks SOA1 and SOA2.

Figure 2 shows a SOA subdivided into two sections by introducing a fictitious boundary at $\xi = L_1$. We name these two sections as SOA1 and SOA2 in the analysis to follow and use subscripts 1 and 2 to represent all the relevant material parameters of SOA1 and SOA2, respectively. Using (34), the overall gain, $G(L_1 + L_2, \mathcal{T}, \mathcal{U})$, can be written as

$$G([0, L_2], \mathcal{T}, \mathcal{U}) = G_1([0, L_1], \mathcal{T}, \mathcal{U}) \times G_2([L1, L_2], \mathcal{T}, \mathcal{U}) \quad (36)$$

where $G_1([0, L_1], \mathcal{T}, \mathcal{U})$ and $G_2([L_1, L_2], \mathcal{T}, \mathcal{U})$ are signal gains of SOA1 and SOA2, respectively with following definitions

$$G_1([0, L_1], \mathcal{T}, \mathcal{U}) = \exp\left(h_{\wp,1}(L_1)\left(1 - \exp(-\mathcal{U})\right)\right) \times \left(1 - \left(1 - \exp\left(-h_{I,1}\left(L_1\right)\right)\right)/E_{\beta,1}(\mathcal{T})\right)^{-\exp(-\mathcal{U})} \quad (37)$$

and

$$G_2([L_1, L_2], \mathcal{T}, \mathcal{U}) = \exp\left(h_{\wp,2}(L_2)\left(1 - \exp(-\mathcal{U})\right)\right) \times \left(1 - \left(1 - \exp\left(-h_{I,2}\left(L_2\right)\right)\right)/E_{\beta,2}(\mathcal{T})\right)^{-\exp(-\mathcal{U})} \quad (38)$$

The total gain $G(L_1 + L_2, \mathcal{T}, \mathcal{U})$, can be written as using the parameters associated with the two sections as

$$G_1([0, L_2], \mathcal{T}, \mathcal{U}) = \exp\left(h_{\wp}\left(1 - \exp(-\mathcal{U})\right)\right) \times \left(1 - \left(1 - \exp\left(-h_{\wp}\right)\right)/E_{\beta,1}(\mathcal{T})\right)^{-\exp(-\mathcal{U})} \quad (39)$$

where $h_{\wp} = h_{\wp,1}(L_1) + h_{\wp,2}(L_2)$. Solving (36), we get following expression for $E_{\beta,2}(\mathcal{T})$

$$E_{\beta,2}(\mathcal{T}) = \exp\left(h_{\wp,1}(L_1)\right) E_{\beta,1}(\mathcal{T}) - \left(\exp\left(h_{\wp,1}(L_1)\right) - 1\right) \quad (40)$$

Combining (40) and (35), we can write the following expression for the Energy Gain, $G_{\mathcal{E}}(\xi, \mathcal{T})$ at time, $\mathcal{T}$ and distance ξ as

$$G_{\mathcal{E}}(\xi, \mathcal{T}) = \frac{\ln\left(\exp\left(h_{\wp}(\xi)\right) E_{\beta}(\mathcal{T}) - \left(\exp\left(h_{\wp}(\xi)\right) - 1\right)\right)}{\ln\left(E_{\beta}(\mathcal{T})\right)} \quad (41)$$

It is interesting note that this expression is equal to the both Agrawal and Olsson [3] and Sieman [17] results with corresponding notation change. However, we arrived at this results using self-consistency arguments of our approximate results, deviating from the physical arguments given in the above papers.

IV. Gain Recovery Dynamics When Waveguide Loss Cannot be Neglected

When the waveguide loss, α, is not negligible, (16) assumes the following form by matching the zeroth order terms (i.e. ϵ^0

$$\frac{\partial}{\partial \mathcal{T}} h_0(\xi, \mathcal{T}, \mathcal{U}) = -\beta(\mathcal{T})\left(\exp\left(h_0(\xi, \mathcal{T}, \mathcal{U}) - \alpha\xi\right) - 1\right) - \alpha\beta(\mathcal{T}) \int_0^{\xi} \exp\left(h_0(\xi, \mathcal{T}, \mathcal{U}) - \alpha\xi\right)\, d\xi \quad (42)$$

and (17) assumes the following form by matching the first order terms (i.e. ϵ^1)

$$\frac{\partial}{\partial \mathcal{T}} h_0(\xi, \mathcal{T}, \mathcal{U}) + \frac{\partial}{\partial \mathcal{U}} h_1(\xi, \mathcal{T}, \mathcal{U}) = \left(h_{\wp} - h_0(\xi, \mathcal{T}, \mathcal{U})\right) - \beta(\mathcal{T}) \exp\left(h_0(\xi, \mathcal{T}, \mathcal{U}) - \alpha\xi\right) h_1(\xi, \mathcal{T}, \mathcal{U}) - \alpha\beta(\mathcal{T}) \int_0^{\xi} h_1(\xi, \mathcal{T}, \mathcal{U}) \exp\left(h_0(\xi, \mathcal{T}, \mathcal{U}) - \alpha\xi\right)\, d\xi \quad (43)$$

It is not possible to solve these equations in the current for due to nonlinear integral terms. Noting that if the gain is uniform along the SOA (i.e. $h_0(\xi, \mathcal{T}, \mathcal{U}) \equiv \bar{h}(\mathcal{T}, \mathcal{U})\,\xi$) for some function $\bar{g}(\mathcal{T}, \mathcal{U})$ independent of spatial coordinate, then we could write the integral in the (42) as

$$\int_0^{\xi} \exp\left(h_0(\xi, \mathcal{T}, \mathcal{U}) - \alpha\xi\right)\, d\xi = \frac{\exp\left(\bar{g}(\mathcal{T}, \mathcal{U})\,\xi - \alpha\xi\right) - 1}{\bar{g}(\mathcal{T}, \mathcal{U}) - \alpha} \quad (44)$$

Noting this, we introduce the following approximation for the above integral when gain distribution is spatially non-uniform

$$\int_0^{\xi} \exp\left(h_0(\xi, \mathcal{T}, \mathcal{U}) - \alpha\xi\right)\, d\xi \approx \frac{\exp\left(h_0(\xi, \mathcal{T}, \mathcal{U}) - \alpha\xi\right) - 1}{\tilde{g}(\xi, \mathcal{T}, \mathcal{U}) - \alpha} \quad (45)$$

where $\tilde{g}(\xi, \mathcal{T}, \mathcal{U})$ is given by

$$\tilde{g}(\xi, \mathcal{T}, \mathcal{U}) = \frac{h_{\wp}(\xi)}{\xi}\left(1 - \exp(-\mathcal{U})\right) - \frac{\ln\left(\left(1 - \left(1 - \exp\left(-h_I\left(\xi\right)\right)\right)/E_{\beta}(\mathcal{T})\right)\right)}{\xi} \exp(-\mathcal{U}) \quad (46)$$

As we show later using simulations, this is a very good approximation for the integral in (45). Substitution of (45) to (42) gives the following modified equation

$$\frac{\partial}{\partial \mathcal{T}} h_0(\xi, \mathcal{T}, \mathcal{U}) = -\frac{\beta(\mathcal{T})\tilde{g}(\xi, \mathcal{T}, \mathcal{U})}{\tilde{g}(\xi, \mathcal{T}, \mathcal{U}) - \alpha}\left(\exp\left(h_0(\xi, \mathcal{T}, \mathcal{U} - \alpha\xi)\right) - 1\right) \quad (47)$$

Noting that in multiple-scales analysis, lower order coefficients of the expansion $h(\xi, \mathcal{T}, \mathcal{U}, \epsilon) = \sum_{n=0}^{\infty} h_n(\xi, \mathcal{T}, \mathcal{U})\,\epsilon^n$ affects higher order but not vice-versa to eliminate secular-terms, we could split (43) into two simultaneous differential equations

$$\frac{\partial}{\partial \mathcal{T}} h_0(\xi, \mathcal{T}, \mathcal{U}) = h_{\wp} - h_0(\xi, \mathcal{T}, \mathcal{U}) \quad (48)$$

TABLE I
PARAMETERS USED IN SIMULATIONS

SOA Length (L)	378.0×10^{-6} m
Active Region Width (w)	2.5×10^{-6} m
Active Region Thickness (d)	0.2×10^{-6} m
Waveguide Group Effective Index (n_g)	3.7
Loss Coefficient (α)	3000.0 m^{-1}
Carrier Recombination Coefficient (τ_e)	300.0×10^{-12} s
Carrier Injection Rate ($\wp$)	1.177×10^{34} $\mathrm{s}^{-1}\mathrm{m}^{-3}$
Confinement Factor (Γ)	0.3
Material Gain Coefficient (a)	2.5×10^{-20} m^2
Transparency Carrier Density (N_0)	1.5×10^{24} m^{-3}
Linewidth Enhancement Factor (α_L)	5.0
Nominal Wavelength (λ)	1552.52×10^{-9} m

$$\frac{\partial}{\partial \mathcal{U}} h_1(\xi,\mathcal{T},\mathcal{U}) = -\beta(\mathcal{T}) \exp\left(h_0(\xi,\mathcal{T},\mathcal{U}) - \alpha\xi\right) h_1(\xi,\mathcal{T},\mathcal{U}) - \alpha\beta(\mathcal{T}) \int_0^{\xi} h_1(\xi,\mathcal{T},\mathcal{U}) \exp\left(h_0(\xi,\mathcal{T},\mathcal{U}) - \alpha\xi\right)\, d\xi \quad (49)$$

Following the same procedure as in Section III and solving the couple equations (47) and (48), the modal gain can be written as

$$\exp\left(h_0(\xi,\mathcal{T},\mathcal{U}) - \alpha\xi\right) = \exp\left(\left(h_\wp(\xi) - \alpha\xi\right)\left(1 - \exp(-\mathcal{U})\right)\right) \times \left(1 - \left(1 - \exp\left(-h_I(\xi) + \alpha\xi\right)\right)/E_\gamma(\mathcal{T})\right)^{-\exp(-\mathcal{U})} \quad (50)$$

where $E_\gamma(\mathcal{T})$ is defined as

$$E_\gamma(\mathcal{T}) = \exp\left(\int_0^{\mathcal{T}} \frac{\beta(\mathcal{T})\tilde{g}(\xi,\mathcal{T},\mathcal{U})}{\tilde{g}(\xi,\mathcal{T},\mathcal{U}) - \alpha}\, d\mathcal{T}\right) \quad (51)$$

In the next Section, we show the accuracy of these expressions by comparing them directly with numerically integrated results.

V. COMPARISON OF ANALYTICAL RESULTS WITH NUMERICALLY INTEGRATED RESULTS

To demonstrate the accuracy of the results derived so far, we compare our analytical results with numerical simulations. Unless specified otherwise, we use parameters given in the Table I for our calculations. The numerical results were generated by directly integrating the coupled equations (2) and (3) in MATLAB™. Throughout our simulations, we use an intensity profile of an unchirped (transform-limited) Gaussian pulse, $I_{T_W}(t)$ with pulse energy, E_{in}, and FWHM value of T_{FWHM}

$$I_{T_w}(t) = \frac{E_{in}}{AT_0\sqrt{\pi}} \exp\left(-\frac{t^2}{T_0^2}\right) \quad (52)$$

where A is the mode area and $T_0 \simeq T_{\mathrm{FWHM}}/1.665$.

Carrier density, N along the SOA can be calculated by noting the relationship between N and h as described in (7). Fig. 3 shows the normalized carrier density, $(N - N_0)/N_0$, against SOA position, z, at elapsed times of: (I) 0.0 ps (II) 100.0 ps and (III) 500 ps, after a Gaussian pulse of 2.0 ps FWHM and energy: (a) $Ein = 50$ fJ and (b) $Ein = 500$ fJ has passed completely through the SOA. The dashed lines (- -) show the numerical simulation results and the solid lines (—) show the carrier density calculated using the analytical solution of (50). Fig. 3 clearly shows that analytical gain approximation (50) has the ability to accurately represent the spatial and temporal gain dynamics for SOAs under different saturation conditions.

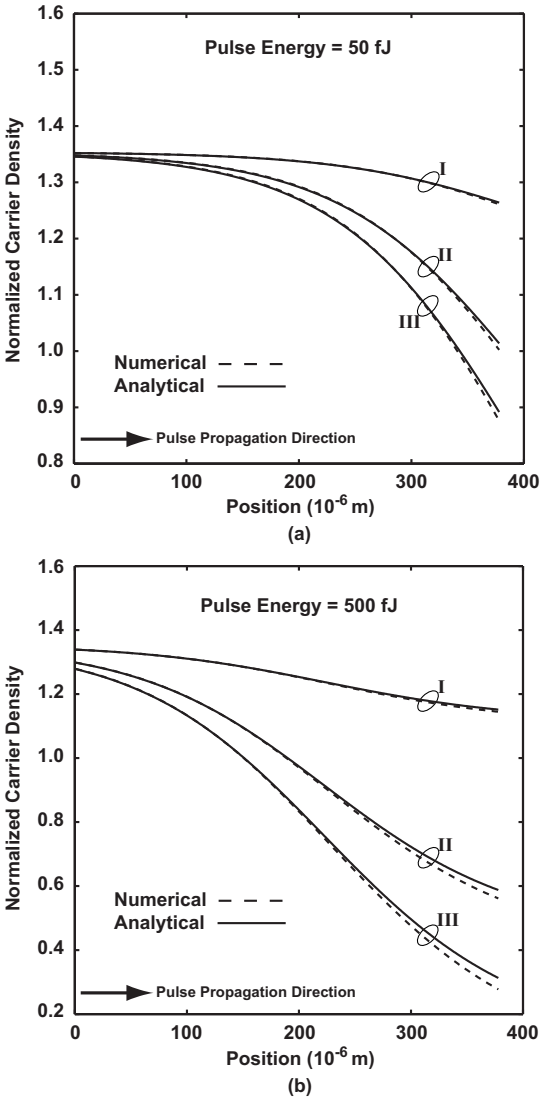

Fig. 3. Normalized carrier density, $(N - N_0)/N_0$, against SOA position, z, at elapsed times of: (I) 0.0 ps (II) 100.0 ps and (III) 500 ps, after a Gaussian pulse of 2.0 ps FWHM and energy: (a) $Ein = 50$ fJ and (b) $Ein = 500$ fJ has passed completely through the SOA.

A much deeper insight into the accuracy and validity of our approximate solution can be obtained by looking at the output pulse shape and pulse spectrum of an amplified pulse. Fig. 4 shows amplified: (a) pulse shape and (b) pulse spectrum of a Gaussian pulse of 20 ps FWHM and energy: (I) 50.0 fJ and (II) 500.0 fJ. The incident frequency is equal to c/λ where c is the speed of light in vacuum. The dashed lines (- -) show the numerical simulation results and the solid lines (—) show the corresponding analytical results. Fig. 4 shows that as the pulse energy increases, the amplified pulse becomes asymmetric such that its leading-edge is sharper compared with the trailing-edge. This is because the leading-edge sees larger gain

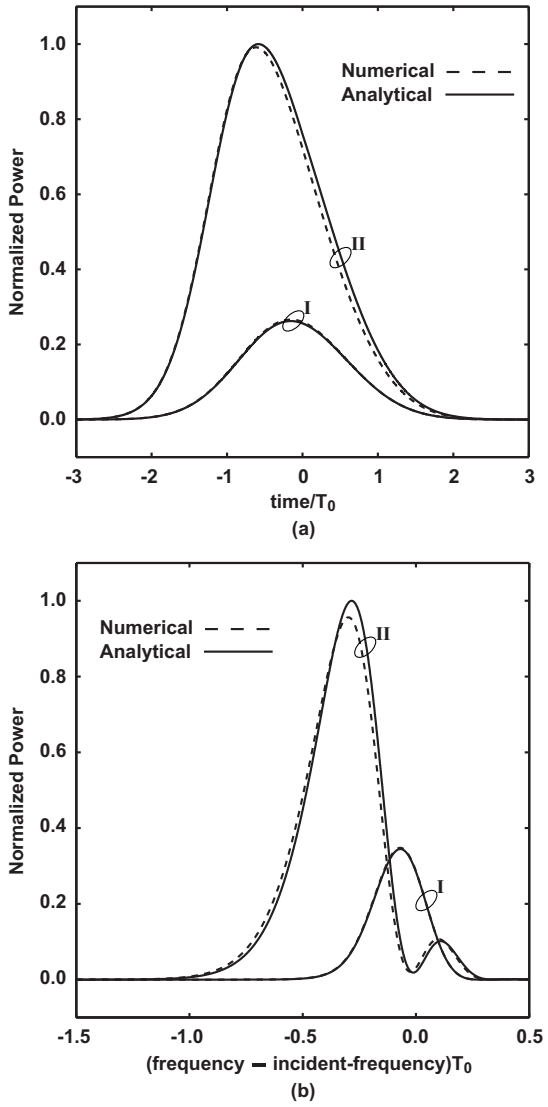

Fig. 4. Amplified: (a) pulse shape and (b) pulse spectrum of a Gaussian pulse of 20 ps FWHM and energy: (I) 50.0 fJ and (II) 500.0 fJ.

than trailing-edge due to the saturation of the gain medium by the photons in the leading-edge. Due to this asymmetry and SPM (self phase modulation) induced frequency chirp on the pulse, the spectrum of the pulse attains a multipeak structure. As clearly seen from Fig. 4, the dominant spectral peak shifts to the low-frequency side (red-shift). The red-shift increases for both higher amplifier gain and higher pulse energy. The asymmetry of the pulse-spectrum is due to the asymmetry in the pulse-shape but the multiple peaks are due to the SPM related interference of frequencies within the pulse. A good match between numerical and analytical results re-confirms the accuracy of the approximate solution.

It is also interesting to investigate how the approximate solution behaves under different waveguide loss conditions. Fig. 5 shows amplified pulse spectrum of an input Gaussian pulse of 20 ps FWHM and 500.0 fJ of energy when loss coefficient of SOA is given by (I) $\alpha = 3000.0\ \mathrm{m}^{-1}$ and (II) $\alpha = 0.0\ \mathrm{m}^{-1}$. The dashed lines (- -) show the numerical simulation results and the solid lines (—) show the corresponding analytical

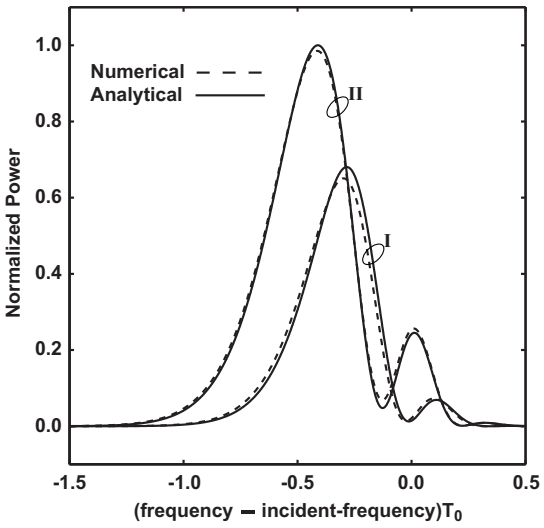

Fig. 5. Amplified pulse spectrum of an input Gaussian pulse of 20 ps FWHM and 500.0 fJ of energy when loss coefficient of SOA is given by (I) $\alpha = 3000.0\ \mathrm{m}^{-1}$ and (II) $\alpha = 0.0\ \mathrm{m}^{-1}$

results. As clearly seen from Fig. 5, the dominant spectral peak red-shift in the low loss (i.e high gain) SOA. Again, a very good match between numerical and analytical results confirms the wide applicability of the approximate solution.

VI. Conclusion

In this paper, we proposed a systematic way to construct approximate solutions for gain recovery dynamics in SOAs using multiple-scales techniques. The main contribution of this work is to put widely used heuristic arguments onto a firm theoretical base so that approximate analytical solutions for carrier recovery dynamics for different variants of SOA models can be systematically constructed. Surpassing previous work in this area, we showed that it is possible to construct analytical solutions to describe gain recovery dynamics when waveguide attenuation is not negligible. By comparing with directly numerically integrated results, we showed that our approximate results can accurately describe the carrier density evolution along the SOA when optical pulses transit through the SOA gain medium. Also, we compared our analytical results against numerical results of amplified pulse-shape and pulse-spectrum for both lossy and lossless SOAs. Very good agreement between numerical and analytical results confirms the wide applicability of the carrier recovery dynamics solution in many practically useful cases.

References

[1] P. G. Eliseev and V. V. Luc, "Semiconductor optical amplifiers: multi-functional possibilities, photoresponse and phase shift properties", *Pure Appl. Opt.*, Vol. 4, pp. 295-313, 1995.

[2] B. Dagens, A. Labrousse, R. Brenot, B. Lavigne, M. Renaud, "SOA-based devices for all-optical signal processing", *Optical Fiber Communications Conference: OFC 2003*, Vol. 2, pp. 582- 583, 2003.

[3] G. P. Agrawal and N. A. Olsson, "Self-phase modulation and spectral broadening of optical pulses in semiconductor laser amplifiers", *IEEE J. Quantum Electron.*, Vol. 25, pp. 2297-2306, 1989.

[4] A. Mecozzi and J. Mork, "Saturation induced by picosecond pulses in semiconductor optical amplifiers", *J. Opt. Soc. Am. B*, Vol. 14, pp. 761-770, 1997.

[5] J.P. Sokoloff, P. R. Prucnal, I. Glesk, M. Kane, "A terahertz optical asymmetric demultiplexer (TOAD)", *Photonic Technol. Letts.*, Vol. 5,pp. 787-790, 1993.
[6] M. Eiselt, W. Pieper, H. G. Weber, "SLALOM: semiconductor laser amplifier in a loop mirror", *J. Lightw. Technol.*, Vol. 13, pp. 2099-2112, 1995.
[7] T. Wang, Z. Li, C. Lou, Y. Wu and Y. Gao, "Comb-like filter preprocessing to reduce the pattern effect in the clock recovery based on SOA", *IEEE Photon Technol. Letts.*, Vol. 14, pp. 855-857, 2002.
[8] M. Weiming, L. Yuhua, A-M. Mohammed,L. Guifang, "All-optical clock recovery for both RZ and NRZ data", *IEEE Photonics Technol. Letters*, Vol. 14, pp. 873-875, 2002.
[9] E. S. Awad, C. J. K. Richardson, P. S. Cho, N. Moulton, and J. Goldhar: "Optical clock recovery using SOA for relative timing extraction between counterpropagating short picosecond pulses", *IEEE Photonics Technol. Letters*, Vol. 14, pp. 396-398, 2002.
[10] M. Premaratne and A. J. Lowery, "Analytical characterization of SOA-based optical pulse delay discriminator", *J. of Lightwave Technol.*, Vol. 23, No. 9, pp. 2778-2787, 2005.
[11] M. Premaratne and A. J. Lowery, "Semiclassical analysis of the impact of noise in SOA-based optical pulse delay discriminator", *IEEE J. Selec. Topics in Quantum Electron.*, Vol. 12, pp. 708-716, 2006.
[12] K. L. Hall and K. A. Rauschenbach, "100-Gbit/s bitwise logic", *Opt. Lett.*, Vol. 23, pp. 1271-1273, 1998.
[13] A. Hamie, A. Sharaiha, M. Guegan and B. Pucel, "All-optical logic NOR gate using two-cascaded semiconductor optical amplifiers", *IEEE Photonics Technol. Letters*, Vol. 14, pp. 1439-1441, 2002.
[14] P. G. Kryukov and V. S. Letokhov, "Propagation of a light pulse in a resonantly amplifying (absorbing) medium", *Sov. Phys. Uspekhi*, Vol. 12, pp. 641-672, 1970.
[15] A. E. Siegman, *Lasers*, University Science Books, Mill Valley, California, 1986.
[16] L. M. Frantz and J. S. Nodvik, "Theory of pulse propagation in a laser amplifier", *J. Appl. Phys.*, Vol. 34, pp. 2346-2349, 1963.
[17] A. E. Siegman, "Design considerations for laser pulse amplifiers", *J. Appl. Phys.*, Vol. 35, pp. 460-461, 1964.
[18] B. S. Gopalakrishna Pillai, Malin Premaratne, D. Abramson, K. L. Lee, A. Nirmalathas, C. Lim, S. Shinada, N. Wada, and T. Miyazaki, Analytical Characterization of Optical Pulse Propagation in Polarization-Sensitive Semiconductor Optical Amplifiers,*IEEE J. Quantum Electronics*, Vol. 42, pp. 1062-1077, 2006.
[19] G. W. Bush, *Perturbation Methods for Engineers and Scientists*, CRC Press, Florida, 1992.
[20] A. H. Nayfeh, *Perturbation Methods*, Wiley-Interscience, New York, 2000.
[21] A. J. Jerri, *Introduction to Integral Equations with Applications*, Second Edition, John Wiley & Sons Inc., New York, 1999.

Malin Premaratne (M'98-SM'03) received the BSc(maths.) and BE(elec.) with first class honors from the University of Melbourne, Australia, in 1995 and Ph.D degree from the same University in 1998.

From 1998 to 2000, he was with the Photonics Research Laboratory, a division of the Australian Photonics Cooperative Research Centre (APCRC), the University of Melbourne, where he was the Coproject Leader of the APCRC Optical Amplifier Project. During this period, he worked with Telstra, Australia and Hewlett Packard, USA through the University of Melbourne. From 2000 to 2003 he was involved with several leading startups in the photonic area either as an Employee or a Consultant. During this period, he has also served in the editorial boards of SPIE/Kluwer and Wiley publishers in the optical communications area. From 2001 to 2003, he worked as the Product Manger (Research and Development) of VPIsystems Optical Systems group. Since 2003, he steered the research program in high-performance computing applications to complex systems simulations at the Advanced Computing and Simulation Laboratory (AXL) at Monash University, where currently he serves as the Deputy Research Director. He has published over 100 research papers in the areas of semiconductor lasers, EDFA and Raman amplifiers, optical network design algorithms and numerical simulation techniques. At present, he holds visiting research appointments with The University of Melbourne, Australian National University, University of California - Los Angeles (UCLA) and University of Rochester, New York. Dr. Premaratne is a Senior Member of IEEE and a Fellow of the Institution of Engineers Australia (FIEAust).

Dr. Premaratne is an executive member of IEAust Victoria Australia and since 2001 had served as the Chairman of IEEE Lasers and Electro-Optics Society in Victoria, Australia.

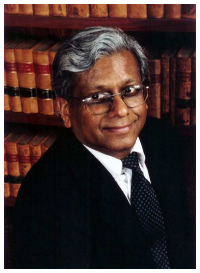

Govind P. Agrawal (M'83-SM'86-F'96) Govind P. Agrawal received the B.S. degree from the University of Lucknow in 1969 and the M.S. and Ph.D. degrees from the Indian Institute of Technology, New Delhi in 1971 and 1974 respectively.

After holding positions at the Ecole Polytechnique, France, the City University of New York, New York, and AT&T Bell Laboratories, Murray Hill, NJ, Dr. Agrawal joined in 1989 the faculty of the Institute of Optics at the University of Rochester, where he is a Professor of Optics. His research interests focus on optical communications, nonlinear optics, and laser physics. He is an author or coauthor of more than 300 research papers, several book chapters and review articles, and seven books entitled: Semiconductor Laser (Norwell, MA: Kluwer Academic, 2nd ed., 1993); Fiber-Optic Communication Systems (Hoboken, NJ: Wiley, 3rd ed., 2002); Nonlinear Fiber Optics (Boston: Academic Press, 4th ed., 2007); Applications of Nonlinear Fiber Optics (Boston: Academic Press, 2001); Optical Solitons: From Fibers to Photonic Crystals (San Diego, CA: Academic Press, 2003); Lightwave Technology: Components and Devices (Hoboken, NJ: Wiley, 2004), and Lightwave Technology: Telecommunication System (Hoboken, NJ: Wiley, 2005). He has participated multiple times in organizing technical conferences sponsored by IEEE and OSA. He was the General Cochair in 2001 for the Quantum Electronics and Laser Science (QELS) Conference and a member of the Program committee in 2004 and 2005 for the Conference on Lasers and Electro-Optics (CLEO).

Dr. Agrawal is a Fellow of both the Optical society of America (OSA) and the Institute of Electrical and Electronics Engineers (IEEE). He is also a Life Fellow of the Optical Society of India.

Dragan Nesic (M'00-SM'02-F'07) Dr. Dragan Nesic is a Professor in the Department of Electrical and Electronic Engineering (DEEE) at The University of Melbourne, Australia. He received his BE degree from The University of Belgrade, Yugoslavia in 1990, and his Ph.D. degree from Systems Engineering, RSISE, Australian National University, Canberra, Australia in 1997. In the period of 1997-1999 he held postdoctoral positions at DEEE, The University of Melbourne, Australia; CESAME, Universit Catholique de Louvain, Louvain la Neuve, Belgium; and ECE, University of California, Santa Barbara, CA, USA. Since February 1999 he has been with The University of Melbourne. His research interests include networked control systems, discrete-time, sampled-data and continuous-time nonlinear control systems, input-to-state stability, extremum seeking control, applications of symbolic computation in control theory, and so on. In 2003 Prof. Nesic was awarded a Humboldt Research Fellowship funded by the Alexander von Humboldt Foundation, Germany. Currently, Prof. Nesic is an Australian Professorial Fellow (2004-2009), which is a research position funded by the Australian Research Council. Prof. Nesic is a Fellow of IEEE and a Fellow of IEAust. He is an Associate Editor for the journals Automatica, IEEE Transactions on Automatic Control, Systems and Control Letters and European Journal of Control.